Nano Research
2021, 14(8): 2589–2595
ISSN 1998-0124 CN 11-5974/O4
https://doi.org/10.1007/s12274-020-3259-x

Research Article

A high-strength self-healing nano-silica hydrogel with anisotropic differential conductivity

Xingyu Huang[1], Xiaofan Zhou[1] (✉), Hao Zhou[1], Yidan Zhong[1], Hui Luo[1], and Fan Zhang[2]

[1] *Jiangsu Co-Innovation Center of Efficient Processing and Utilization of Forest Resources, Jiangsu Provincial Key Lab of Pulp and Paper Science and Technology, College of Light Industry and Food, Nanjing Forestry University, Nanjing 210037, China*
[2] *Department of Creative Design, Zhicheng College, Fuzhou University, Fuzhou 350000, China*

Received: 7 November 2020 / **Revised:** 19 November 2020 / **Accepted:** 22 November 2020

ABSTRACT

Soft nano electronic materials based on conductive hydrogels have attracted considerable attention due to their exceptional properties. Particle deposition and poor interface compatibility often diminish the mechanical strength and electron transport capabilities of the conductive hydrogel. Mechanical damage can severely impact the performance of the conductive hydrogel and can even damage electronic devices based on the conductive hydrogel. In the current study, a transparent nano-silica hydrogel is prepared by employing an extremely easy-to-operate method. This approach can preclude the deposition of particles via strong mechanical force. In addition, controlling the concentration of the reaction interface makes the hydrogel grow along the mechanical force in the direction with a special directional hole structure formed. The hydrogel is transparent, showing excellent self-healing properties—it can self-heal within 15 seconds. Remarkably, the hydrogel after self-healing maintains its performance. Moreover, it has excellent mechanical properties and can be stretched in length. Up to 1,200% of the original length, the tensile strength of the gel spline can reach 7 MPa. The viscosity of the hydrogel can reach 1.67×10^8 (MPs). In addition, a large amount of Na^+ in this hydrogel endow it a conductivity of 389 μs/cm. The conductivity of this hydrogel is adjustable result from the special pore structure. Lastly, the difference between the horizontal and vertical conductivity of the same sample can reach 3–4 times, thus this hydrogel can be used in the field of nano conductive materials.

KEYWORDS

self-healing; nanosilica; hydrogels; anisotropic conductivity

1 Introduction

Nano-structured soft electronic materials have received widespread attention due to their novel properties [1]. Conductive hydrogels combine the mechanical properties of the hydrogel and the electrical properties of the conductor. They display characteristics of high stretchability, self-repairing ability, fast responsiveness, and good electrochemical performance. Conductive hydrogels have 3D layered porous network structures, thus promoting the transportation of electrons and charges as well as the diffusion of ions and molecules. However, particle deposition and poor interface compatibility diminish the mechanical strength and electron transport capabilities of the conductive hydrogel. These conductive hydrogels are opaque and can provoke irreversible effects in practical applications. Mechanical damage can severely impact the performance of conductive hydrogels, and even damage electronic devices from conductive hydrogels [2–8].

It remains a challenge to synthesize self-healing transparent hydrogels with required electronic properties and good mechanical properties [9]. The self-repair mechanism of hydrogels is reversibly cross-linking, and there are two main combinations—reversible covalent bonds such as imine bonds, and reversible non-covalent bonds such as hydrogen bonds [10–14]. Different from traditional hydrogels, self-healing hydrogels can repair themselves after damage [15–16]. For example, a physically cross-linked hydrogel is prepared by hydrogen and a double metal carboxylate coordination bond. The obtained hydrogel possesses good mechanical strength and self-healing properties [17]. Wei and his colleagues synthesized a highly stretchable and self-healing hydrogel. Due to electrostatic interactions, the resulting hydrogels present high hardness and good cohesion [18]. Jiang et al. prepared a hydrogel based on agarose/PVA dual network by dynamic borate bonding. Consequently, the hydrogel has ultra-fast self-healing properties even in water [19]. The above-mentioned self-healing hydrogels with better properties are all dual-network hydrogels or contain organic components. In contrast, relatively few studies on this type of inorganic self-healing hydrogel have been reported [20–38]. Researchers have proposed the self-healing properties of nanoparticles. For example, the nano Si–Sn composite additive prepared by Dong et al. can significantly enhance the repair effect of the worn surface of the HV1500 base oil [39].

Learning from previous research, we decided to use a very cheap sodium silicate as a raw material to prepare nano-SiO_2 hydrogel in the present study. As an extensively applied material, nano-SiO_2 has been used in various production and many fields in our lives. The pure inorganic gel material composed of SiO_2 nanoparticles has good thixotropy, mechanical strength and biocompatibility. Due to the characteristics of

Address correspondence to refueleveryday@126.com

large particle size, high surface energy, and large specific surface area, when the matrix material has microcracks and damages, nanoparticles can effectively locate and repair the microcracks and the damaged area, thereby realizing polymer matrix materials and the enhancement of the maintenance [40, 41]. The use of inexpensive sodium silicate as a raw material can save costs to a large extent.

Our nano SiO_2 hydrogel prepared by a very simple method has excellent self-healing properties, good mechanical properties and anisotropic electrical conductivity. The mechanism of this facile method is curing into glue. To prevent the particles from coalescing, the concentration is constantly adjusted while adding the catalyst. The curing agent can speed up the sol gel process and endows the gels with high mechanical strength. Consequently, it can ensure that the product has the characteristics of a gel with good mechanical properties, and hydrogen bonds between nanoparticles allow the gel being able to quickly repair itself. Different from existing high-strength hydrogels, this hydrogel has both high strain performance and high tensile stress. Through the combination of these characteristics, the gel has great potential in the fields of electrochemistry, supercapacitors, and directional conductive diodes.

2 Experimental

2.1 Materials

Sodium silicate was supplied by Yatai United Chemical Co. LTD (Wuxi, China), Sulfuric acid (98 wt.%) was supplied by Nanjing Chemical Reagent Co. LTD (Nanjing, China). All the chemicals used in the study were of analytical grade and without further refinement.

2.2 Preparation of hydrogels

The high-efficiency procedure for preparing nano-silica hydrogel through concentration control and auxiliary mechanical force is as follows: after sodium silicate is filtered to remove impurities, Pour it into a reaction vessel with a rotation speed of 3,000 r/min. Then, configure sulfuric acid and deionized (DI) water in a ratio of 1:4. The two were added to the reaction system in the proportion of 1:4 each time by a Pipet-Aid. The interval between each addition is 2 min. Then, the mixed solution was continuously stirred for 20 min to form a homogeneous sol. The sol was allowed to stand for 12 hours to form a nano-silica hydrogel. The concentration of the nano-silica hydrogel obtained at this time was 80%. The hydrogel was placed in a high-temperature drying oven and heated at 50 °C. Then, the concentration of the obtained nano-silica is reduced but the strength is greatly improved.

2.3 Characterization

The morphology of nano-silica hydrogel was measured by scanning electron microscope (SEM, JSM-7600F, Japanese Institute of Electronics, Japan). Fourier transform infrared spectroscopy (FT-IR) was performed on Syme6700 spectrometer. X-ray diffraction (XRD) was recorded on a multifunctional horizontal X-ray diffractometer (D8 advanced diffractometer purchased from Bruker). Elemental analysis and mapping were performed by using an environmental scanning electron microscope (Quanta 250 FEG). The rheological properties are measured by RS6000 rheometer (HAAKER, Germany) equipped with P20Til flakes and intervertebral discs. The electrical conductivity of the hydrogel is measured by a Keithley resistance tester (Keithley).

3 Results and discussion

3.1 Preparation process and mechanism

Figure 1 illustrates the synthesis process and mechanism of an inorganic self-healing transparent hydrogel with directional pore structure. Add an appropriate amount of sodium silicate to the reaction vessel. Adjust the power of the mixer to 3000 r/min. Sulfuric acid (98 wt.%) and distilled water are weighed in a ratio of 1:4. Then the two were added to the reaction system in the proportion of 1:4 each time by a Pipet-Aid. The interval between each addition is 2 min. During this process, the concentration of the entire solution will be continuously adjusted. By controlling the viscosity of the solution, after the acid is added, the surrounding substances will react to form a thin film instantly. At the same time, it exerts mechanical force in the same direction to prevent the formation of particle agglomeration. In this process, the reaction system is a highly dispersed system with small dispersed particles and strong Brownian motion, which can prevent the sinking caused by gravity. The SiO_2 produced by the reaction will grow along the direction of mechanical force. During the growth of long-chain molecules, the agglomeration force of the particles will become smaller and smaller, and the required viscosity will also decrease. Until the value is controlled in the range of PH = 8.5 (± 0.5). After standing and aging, SiO_2 hydrogel with oriented pore structure and attached nano pores is finally obtained (Figs. 1(a) and 1(b)). In this process, through strong mechanical force, the hydroxyl and silicon–oxygen double

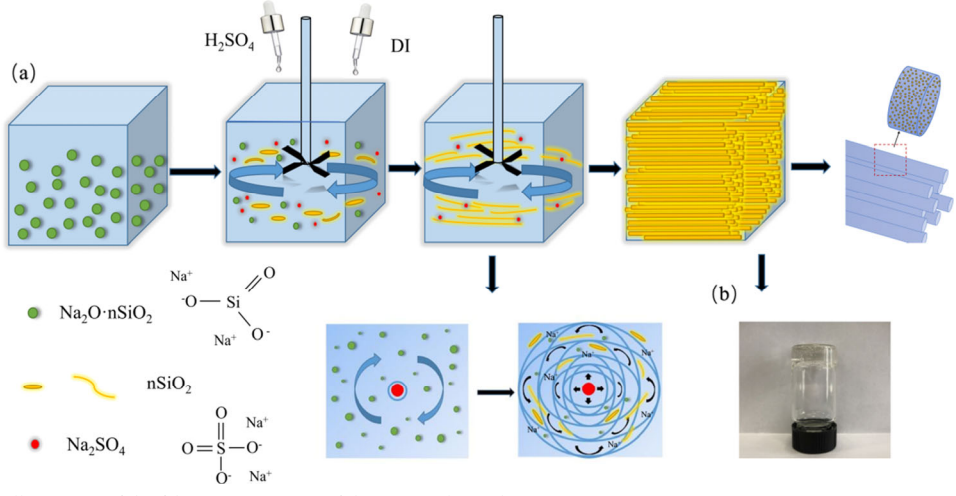

Figure 1 Schematic illustration of the fabrication process of the nano–silica gel.

bond in the generated silicic acid are destroyed. The reaction speed is different due to the difference in concentration. Large pores are generated in the low concentration area, and small pores are generated in the high concentration area. Therefore, the resulting gel has directional macropores with nano pores attached to it. However, because the mechanical force is directional, a silica hydrogel with a pipe-shaped pore structure is finally formed.

3.2 Structure and water retention properties

The shape of the hydrogel is shown in Fig. 2. The transparent hydrogel can be changed into different shapes (Fig. 2(a)). There is a difference between the hydrogel prepared in this work and the ordinary SiO_2 hydrogel after freeze drying. The hydrogel prepared in this article shows transparent properties (Fig. 2(b)). The hydrogel is almost transparent after drying, which indicates that the pores are too small for the moisture to dry. Figure 2(c) is the FT-IR spectrum of the sample. It can be seen that the strong absorption peak at 3,422 cm^{-1} corresponds to the –OH tensile vibration on the sample surface. The absorption peak corresponds to the bending vibration of water molecules. The absorption peak at 1,452 cm^{-1} corresponds to the in-plane bending vibration of –OH. These three peaks prove the presence of hydroxyl groups in the sample. The strong and broad absorption peak at 1,143 cm^{-1} indicates the tensile vibration of the top Si–O bond, while the absorption peak at about 1,000 cm^{-1} corresponds to the flexural vibration absorption peak of Si–OH. These two peaks indicate the presence of silica in the sample. In addition, the absorption peaks at 622 and 468 cm^{-1} correspond to the vibrational absorption peaks of SO_4^{2-}, and these two peaks mainly come from sodium sulfate in the sample. It can be seen from the above analysis that FT-IR can determine the chemical composition of the sample, such as silica, sodium sulfate, and water. Figure 2(d) is the analysis diagram obtained when the sample is irradiated with CuK in the diffraction angle range of 10–50°, scanning speed of 1 °/min. It can be seen from the figure that the X–ary diffraction (XRD) peak of the sample is completely consistent with the standard spectra of Na_2SO_4 (Joint Committee on Powder Diffraction Standards #74-2036) and SiO_2 (JCPDS#80-2147), which confirms the successful synthesis of the SiO_2-NA_2SO_4 sample. The XRD pattern of the sample shows that there are almost no impurity peaks, indicating that under this synthesis condition, there is no excessive raw material residue or side reaction products, and the sample has high purity. The sample in 2 theta value 10–50° has several obvious characteristic peaks, at 19.1°, 23.4°, 28.1°, 28.9°, 32.0°, 33.9°, 38.7°, 48.8°, respectively, corresponds to Na_2SO_4 (111), (220), (131), (040), (311), (022), (222), and (351) crystal plane diffraction peak characteristics. Among them, the strongest diffraction peak appears at 32.0°, which corresponds to the characteristic diffraction peak of the Na_2SO_4 (311) crystal plane. In addition, the characteristic diffraction peaks of the (100), (011), (110), and (112) crystal planes in the sample correspond to SiO_2, which appear at 19.7°, 25.2°, 34.7°, 46.9°, respectively, with low intensity. Compared with Na_2SO_4, according to existing knowledge, the sharper the shape of the diffraction peak and the higher the intensity, the better the crystallinity of the crystal. Therefore, it can be concluded that the SiO_2-Na_2SO_4 samples prepared by this method have high crystallinity, complete crystal structure and high material stability. Figure 2(e) shows that the change trend of the viscosity of the system

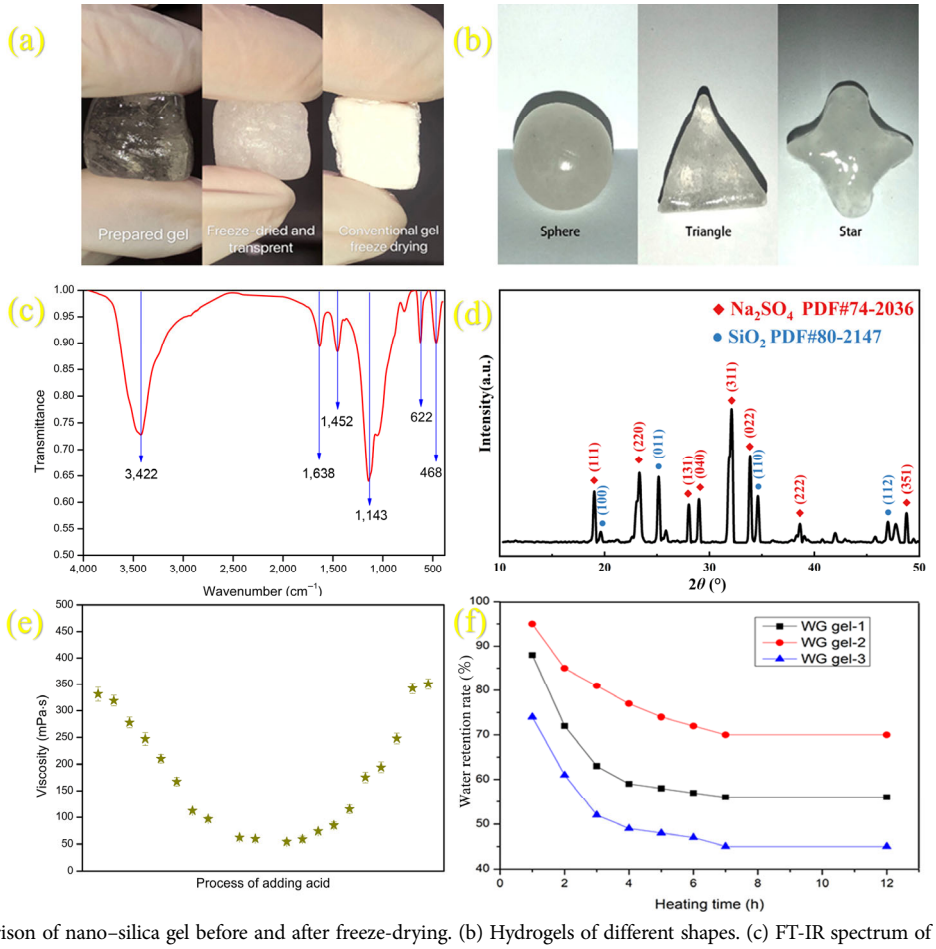

Figure 2 (a) Comparison of nano–silica gel before and after freeze-drying. (b) Hydrogels of different shapes. (c) FT-IR spectrum of the hydrogel. (d) XRD pattern of the hydrogel. (e) The viscosity changes of the reaction system during the formation of the hydrogel. (f) Water retention rate of hydrogel at 105 °C.

during the reaction is a curve relationship that first drops and then rises. It must be ensured that the minimum viscosity of the reaction system is greater than a fixed value. In this experiment, the minimum viscosity is 50 mPa·s. Figure 2(f) detects the changing law of the water retention rate of the hydrogel under different initial concentrations. Place the gel sample in the crucible, and then set the electric heating constant temperature blast drying oven (DHG-9070A, Shanghai Jinghong Experimental Equipment Co., Ltd.) to 105 °C. Put the crucible in the crucible and measure the weight every hour until the weight is constant. The test samples are divided into five groups, and each group is tested three times and the average measured value is obtained.

$$1-\frac{(M-mt)}{M}n$$

Where n is the water retention rate (%), M is the original mass of gel after solidification (g), mt is the mass of gel at the time instant (g).

As shown in the figure, after drying in an electric heating constant temperature blast drying oven at 105 °C for 7 hours, 10%–20% of the water in the gel has not evaporated yet. The sample continued to dry without loss of weight. The main reason is that there are nano pores in the gel, which partially encapsulate water. These holes make the water easy to fix and not easy to lose, so it has good water retention performance.

3.3 Morphology

Figure 3 is a picture of the freeze-dried sample taken through SEM images. As shown in Fig. 3(a), the pore radius of the gel is about 1–2 μm, the arrangement is neat and the direction is uniform. At the same time, there are many interwoven holes connected to the walls of these holes. The figure shows that the pore size of these small holes is in the range of about 5–30 nm. This indicates that the gel 3D pipeline support structure is the reason for the gel's good mechanical properties. Figure 3(b) is the X–ray energy spectrum analysis diagram of the sample, indicating that the main elements in the sample are Si, Na, and O. In order to verify the high strength properties of the gel, the gel was heated at room temperature. The muffle furnace was heated at 300 °C for 4 hours. The scanning electron microscope image of the obtained aerogel is shown in Fig. 4. (a1), (a2) is the sample surface, (a3) is the cross-section of the sample. The resulting aerogel still shows the orientation. The pore structure of the tube, the load pore range is between 20–50 nm. The gel does not shrink at high temperatures. Therefore, the nanopores do not deform during the drying process, which proves that the gel has excellent strength.

3.4 Self-healing properties

Through further observation, it is found that the nano-silica hydrogel shows especially excellent self-healing ability. As shown in Fig. 5(a), the size of the hydrogel is Φ1 × 4.5 cm, and then cut in half. After being exposed to air for 10 seconds, the hydrogel will spontaneously heal into a complete hydrogel and will not be damaged under load. In order to better describe the self-healing ability of the hydrogel, a segment of the nano-silica hydrogel was dyed, and then the undyed nano-silica hydrogel was exposed to the air. The boundary was very obvious at the beginning, and after 10 seconds, their surfaces adhered to

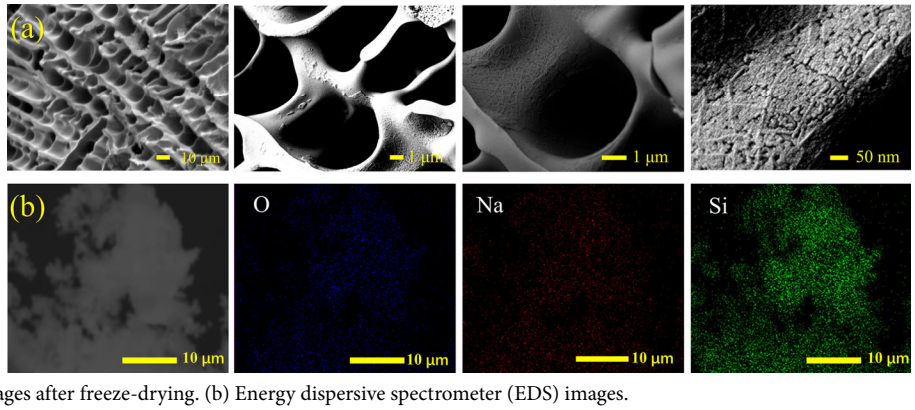

Figure 3 (a) SEM images after freeze-drying. (b) Energy dispersive spectrometer (EDS) images.

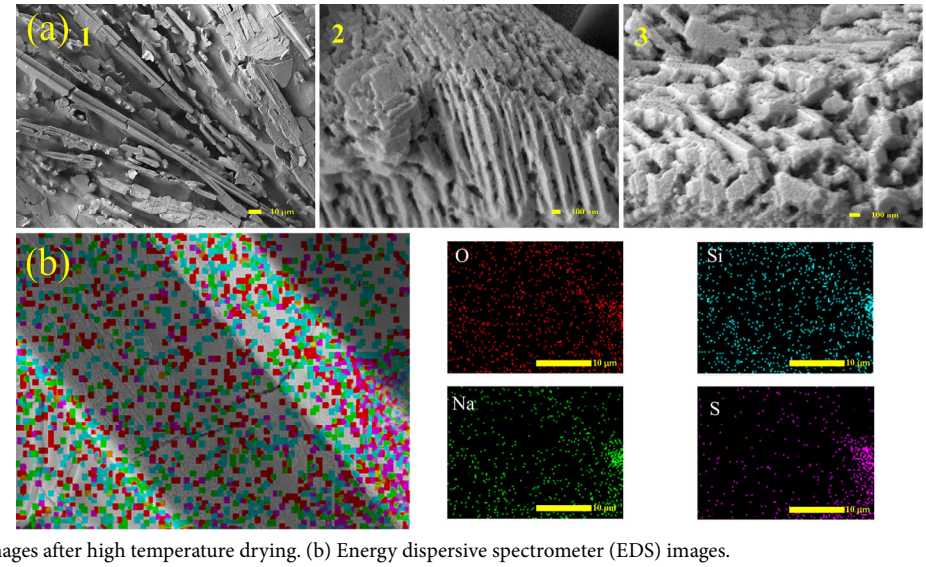

Figure 4 (a) SEM images after high temperature drying. (b) Energy dispersive spectrometer (EDS) images.

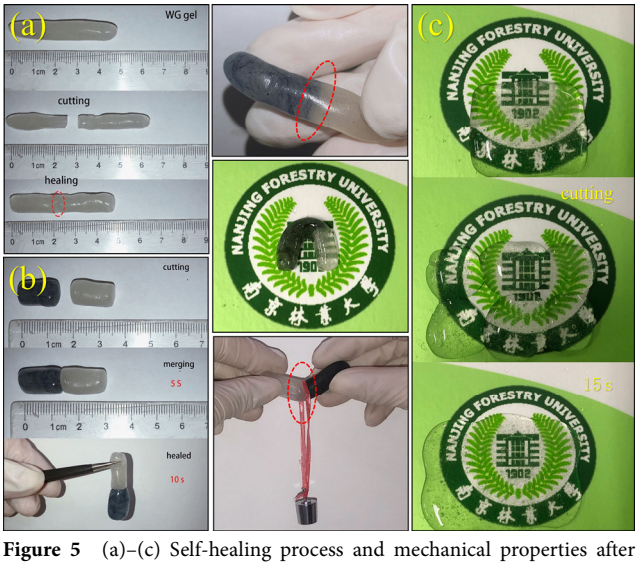

Figure 5 (a)–(c) Self-healing process and mechanical properties after self-healing

each other Tightly. At the same time, the self-healing hydrogel can still bend and load. As shown in Fig. 5, after cutting the hydrogel into six segments, they are automatically repaired in the same way. This indicates that the hydrogel has excellent self-repairing ability. There are two factors here, one is the existence of nano-silica, and the other is the existence of a large number of hydrogen bonds between molecules.

3.5 Mechanical properties

In addition, the hydrogel after self-repair still maintains good mechanical properties. From the comparison between Figs. 6(a) and 6(b), it can be seen that nano-silica hydrogel has good tensile properties before and after self-healing. Both of these hydrogels can be stretched to a strain above 1200% and become thin strips without damage. Both show excellent ductility, destructive resistance and effective energy consumption. Control the moisture content of the original samples of water glass, nano-silica gel and self-healing nano-silica gel, then compress them into pieces in a hot press and test them in a universal testing machine. The resulting tensile strength is shown in Fig. 6(c). The strength of the cured nano-silica gel is slightly lower than the strength before healing, but far exceeds the tensile strength of the water glass itself. This shows that the self-healing nano-silica gel still has good mechanical properties.

Hydrogels generally exhibit properties such as elasticity and viscosity. In different processes, the corresponding storage modulus G' and loss modulus G" performance is viscoelasticity. The result of stress scanning on the prepared gel is shown in Fig. 6(d), G' and G" respectively correspond to the elasticity and viscosity characteristics of the material. The storage modulus (G') of the experimentally prepared nano-silica gel is higher than its loss modulus (G"), showing typical gel characteristics, which is due to the pore size in the gel. The structure distributes through the entire gel network, increasing the overall rigidity of the gel. As shown in Fig. 6(e), the viscoelasticity of the hydrogel sample is in the range of

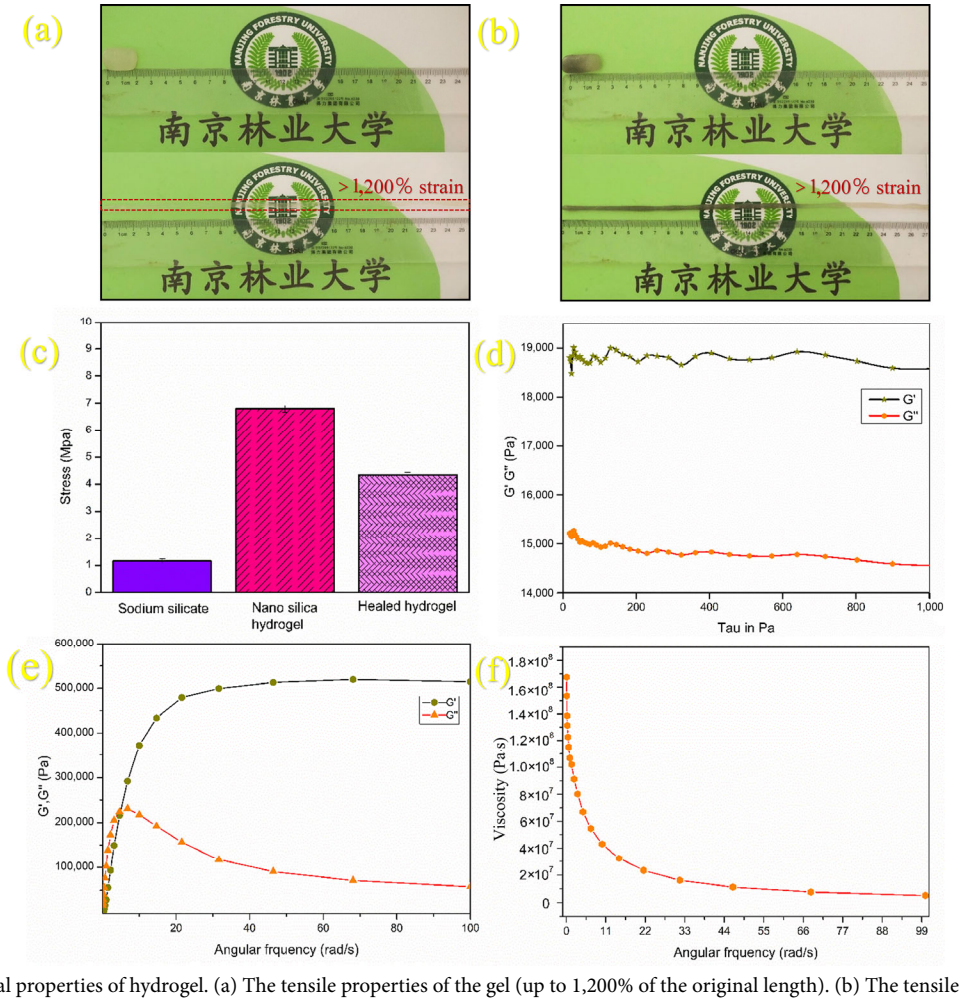

Figure 6 Mechanical properties of hydrogel. (a) The tensile properties of the gel (up to 1,200% of the original length). (b) The tensile properties of the gel after self-healing (up to 1,200% of the original length). (c) Tensile strength. (d) elastic modulus of hydrogels. (e) The viscoelasticity of the sample changes in the range of 0.1–100 rad/s. (f) The viscosity and shear rate of the hydrogel sample as a function.

0.1–100 rad/s. The sample can reach up to 0.514 MPa. According to the hydrogel sample, the modulus curve trend, a rough estimate of the cross-point hydrogel ω = 5 rad/s, G' (ω) and G" (ω) are approximately 220 kPa. Figure 6(f) shows the strength and shear rate of the viscous hydrogel sample is a function. The viscosity of the sample can reach 1.67 × 10^8 mPs. Therefore, the hydrogel prepared by this method has good mechanical properties.

3.6 Anisotropic conductivity

The original nano-silica hydrogel and the self-healing nano-silica hydrogel were tested for resistivity by a multimeter. The indications are 4.083 and 4.276 MΩ, respectively. It shows that the influence of loss on the hydrogel is relatively small (Fig. 7(a)). Figure 7(b) shows the different conductivity of the same gel block in different directions, and the difference can reach 3–4 times in the samples of this study. This is very useful in the field of electrochemistry. Figure 7(c) shows the gel resistivity measured by a Keithley resistivity tester and the gel conductivity calculated by formula conversion. Figure 7(d) shows the connection of nano-silica gel to the circuit. Experiments show that, according to the sealing performance and binding force of the gel, the gel has a certain degree of conductivity, which directly affects the smoothness of the ring. Experimental results show that the hydrogel has electrochemical properties with different orientations. This is because the hydrogel itself has a special directional pore structure. So in the direction of the pore structure, the hydrogel has good conductivity. In the direction perpendicular to the pore structure, poor conductivity is observed. Performance. Further exploration will have good application prospects in supercapacitors, battery separators, and bionic skin.

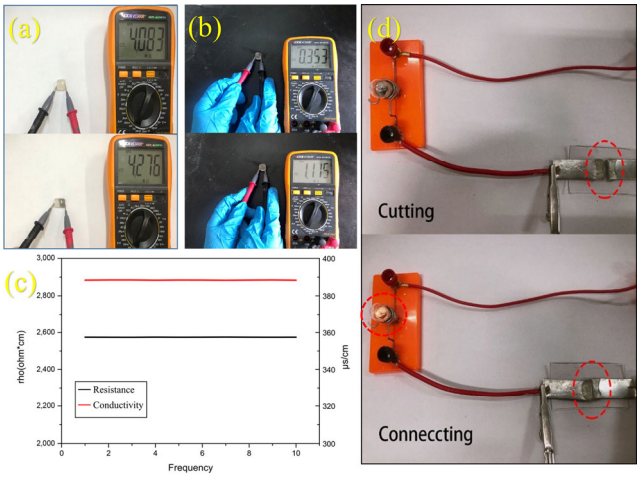

Figure 7 The potential application of hydrogel electrochemistry. (a) Electrical conductivity of the gel and the self-healed gel measured with a multimeter. (b) The use of a multimeter to measure the conductivity of the same gel in different directions. (c) Resistivity and converted conductivity measured by Keithley's resistivity tester. (d) Influence of the opening and closing of the gel on the circuit.

4 Conclusion

In conclusion, we report a simple yet novel method to prepare nano-silica hydrogel materials. Sodium silicate is used as an inexpensive raw material to make high-valued resulting products. The obtained hydrogel material displays anisotropic conductivity. The conductivity difference existing in different directions can reach 3–4 times. The current research can pave a way for the pure inorganic self-healing hydrogel system. In addition, the simple and effective strategies proposed in this research provide new insights and opportunities for manufacturing new products. Furthermore, we could expand their applications to the field of electrochemistry.

Acknowledgements

This work was funded by the Natural Science foundation of Jiangsu provincial University (16KJA220005). This research did not receive any specific grant from funding agencies in the public, commercial, or not-for-profit sectors.

References

[1] Zhao, Y.; Liu, B. R.; Pan, L. J.; Yu, G. H. 3D nanostructured conductive polymer hydrogels for high-performance electrochemical devices. *Energy Environ. Sci.* **2013**, *6*, 2856–2870.

[2] Wang, K.; Zhang, X.; Li, C.; Sun, X. Z.; Meng, Q. H.; Ma, Y. W.; Wei, Z. X. Chemically crosslinked hydrogel film leads to integrated flexible supercapacitors with superior performance. *Adv. Mater.* **2015**, *27*, 7451–7457.

[3] Jin, X. T.; Sun, G. Q.; Zhang, G. F.; Yang, H. S.; Xiao, Y. K.; Gao, J.; Zhang, Z. P.; Qu, L. T. A cross-linked polyacrylamide electrolyte with high ionic conductivity for compressible supercapacitors with wide temperature tolerance. *Nano Res.* **2019**, *12*, 1199–1206.

[4] Lei, Z. Y.; Wang, Q. K.; Sun, S. T.; Zhu, W. C.; Wu, P. Y. A bioinspired mineral hydrogel as a self-healable, mechanically adaptable ionic skin for highly sensitive pressure sensing. *Adv. Mater.* **2017**, *29*, 1700321.

[5] Liu, K.; Pan, X. F.; Chen, L. H.; Huang, L. L.; Ni, Y. H.; Liu, J.; Cao, S. L.; Wang, H. P. Ultrasoft self-healing nanoparticle-hydrogel composites with conductive and magnetic properties. *ACS Sustainable Chem. Eng.* **2018**, *6*, 6395–6403.

[6] Shi, Y.; Zhang, J.; Pan, L. J.; Shi, Y.; Yu, G. H. Energy gels: A bio-inspired material platform for advanced energy applications. *Nano Today* **2016**, *11*, 738–762.

[7] Tian, M.; Chen, X.; Sun, S. T.; Yang, D.; Wu, P. Y. A bioinspired high-modulus mineral hydrogel binder for improving the cycling stability of microsized silicon particle-based lithium-ion battery. *Nano Res.* **2019**, *12*, 1121–1127.

[8] Huang, Y.; Zhong, M.; Huang, Y.; Zhu, M. S.; Pei, Z. X.; Wang, Z. F.; Xue, Q.; Xie, X. M.; Zhi, C. Y. A self-healable and highly stretchable supercapacitor based on a dual crosslinked polyelectrolyte. *Nat. Commun.* **2015**, *6*, 10310.

[9] Meng, F. L.; Zhong, H. X.; Yan, J. M.; Zhang, X. B. Iron-chelated hydrogel-derived bifunctional oxygen electrocatalyst for high-performance rechargeable Zn–air batteries. *Nano Res.* **2017**, *10*, 4436–4447.

[10] Shi, Z. J.; Gao, X.; Ullah, M. W.; Li, S. X.; Wang, Q.; Yang, G. Electroconductive natural polymer-based hydrogels. *Biomaterials* **2016**, *111*, 40–54.

[11] Deng, G. H.; Li, F. Y.; Yu, H. X.; Liu, F. Y.; Liu, C. Y.; Sun, W. X.; Jiang, H. F.; Chen, Y. M. Dynamic hydrogels with an environmental adaptive self-healing ability and dual responsive sol-gel transitions. *ACS Macro Lett.* **2012**, *1*, 275–279.

[12] Gaina, C.; Ursache, O.; Gaina, V.; Varganici, C. D. Thermally reversible cross-linked poly(ether-urethane)s. *Exp. Polym. Lett.* **2013**, *7*, 636–650.

[13] Wang, Y. Q.; Ding, Y.; Guo, X. L.; Yu, G. H. Conductive polymers for stretchable supercapacitors. *Nano Res.* **2019**, *12*, 1978–1987.

[14] Shi, L. Y.; Wang, F. L.; Zhu, W.; Xu, Z. P.; Fuchs, S.; Hilborn, J.; Zhu, L. J.; Ma, Q.; Wang, Y. J.; Weng, X. S. et al. Self-healing silk fibroin-based hydrogel for bone regeneration: Dynamic metal-ligand self-assembly approach. *Adv. Funct. Mater.* **2017**, *27*, 1700591.

[15] Chen, X. Y.; Fan, M.; Tan, H. P.; Ren, B. W.; Yuan, G. L.; Jia, Y.; Li, J. L.; Xiong, D. S.; Xing, X. D.; Niu, X. H. et al. Magnetic and self-healing chitosan-alginate hydrogel encapsulated gelatin microspheres via covalent cross-linking for drug delivery. *Mater. Sci. Eng. C Mater. Biol. Appl.* **2019**, *101*, 619–629.

[16] Lamboni, L.; Gauthier, M.; Yang, G.; Wang, Q. Silk sericin: A versatile material for tissue engineering and drug delivery. *Biotechnol. Adv.* **2015**, *33*, 1855–1867.

[17] Shao, C. Y.; Chang, H. L.; Wang, M.; Xu, F.; Yang, J. High-strength, tough, and self-healing nanocomposite physical hydrogels based on the

synergistic effects of dynamic hydrogen bond and dual coordination bonds. *ACS Appl. Mater. Interfaces* **2017**, *9*, 28305−28318.
[18] Pu, W. F.; Jiang, F.; Chen, P.; Wei, B. A POSS based hydrogel with mechanical robustness, cohesiveness and a rapid self-healing ability by electrostatic interaction. *Soft Matter* **2017**, *13*, 5645−5648.
[19] Chen, W. P.; Hao, D. Z.; Hao, W. J.; Guo, X. L.; Jiang, L. Hydrogel with ultrafast self-healing property both in air and underwater. *ACS Appl. Mater. Interfaces* **2018**, *10*, 1258−1265.
[20] You, B. H.; Li, Q. T.; Dong, H.; Huang, T.; Cao, X. D.; Liao, H. Bilayered HA/CS/PEGDA hydrogel with good biocompatibility and self-healing property for potential application in osteochondral defect repair. *J. Mater. Sci. Technol.* **2018**, *34*, 1016–1025.
[21] Chen, X. L.; He, M. M.; Zhang, X. H.; Lu, T.; Hao, W. Z.; Zhao, Y. S.; Liu, Y. M. Metal-free and stretchable conductive hydrogels for high transparent conductive film and flexible strain sensor with high sensitivity. *Macromol. Chem. Phys.* **2020**, *221*, 2000054.
[22] Sun, Y.; Ren, Y. Y.; Li, Q.; Shi, R. W.; Hu, Y.; Guo, J. N.; Sun, Z.; Yan, F. Conductive, stretchable, and self-healing ionic gel based on dynamic covalent bonds and electrostatic interaction. *Chin. J. Polym. Sci.* **2019**, *37*, 1053–1059.
[23] Lee, J.; Kwon, H.; Seo, J.; Shin, S.; Koo, J. H.; Pang, C.; Son, S.; Kim, J. H.; Jang, Y. H.; Kim, D. E. et al. Conductive fiber-based ultrasensitive textile pressure sensor for wearable electronics. *Adv. Mater.* **2015**, *27*, 2433–2439.
[24] Zhang, L. L.; Zhang, Q.; Yu, J.; Ma, J. X.; Wang, Z. G.; Fan, Y. M.; Kuga, S. Strengthened cellulosic gels by the chemical gelation of cellulose via crosslinking with TEOS. *Cellulose* **2019**, *26*, 9819–9829.
[25] Bian, H. Y.; Wei, L. Q.; Lin, C. X.; Ma, Q. L.; Dai, H. Q.; Zhu, J. Y. Lignin-containing cellulose nanofibril-reinforced polyvinyl alcohol hydrogels. *ACS Sustainable Chem. Eng.* **2018**, *6*, 4821–4828.
[26] Chalitangkoon, J.; Wongkittisin, M.; Monvisade, P. Silver loaded hydroxyethylacryl chitosan/sodium alginate hydrogel films for controlled drug release wound dressings. *Int. J. Biol. Macromol.* **2020**, *159*, 194–203.
[27] Zhu, L. T.; Zong, L.; Wu, X. C.; Li, M. L.; Wang, H. S.; You, J.; Li, C. X. Shapeable fibrous aerogels of metal-organic-frameworks templated with nanocellulose for rapid and large-capacity adsorption. *ACS Nano* **2018**, *12*, 4462–4468.
[28] Yamamoto, T.; Tayakout-Fayolle, M.; Iimura, K.; Satone, H.; Kakibe, T.; Itoh, K.; Maeda, K. Effect of high pressure on growth of colloidal particles during sol-gel phase transition of resorcinol-formaldehyde solution. *Adsorption* **2019**, *25*, 1115–1120.
[29] Li, Y. S.; Hu, X. M.; Cheng, W. M.; Shao, Z. A.; Xue, D.; Zhao, Y. Y.; Lu, W. A novel high-toughness, organic/inorganic double-network fire-retardant gel for coal-seam with high ground temperature. *Fuel* **2020**, *263*, 116779.
[30] Chen, T.; Zhang, S. H.; Lin, Q. H.; Wang, M. J.; Yang, Z.; Zhang, Y. L.; Wang, F. X.; Sun, L. N. Highly sensitive and wide-detection range pressure sensor constructed on a hierarchical-structured conductive fabric as a human–machine interface. *Nanoscale* **2020**, *12*, 21271–21279.
[31] Liang, Y. P.; Zhao, X.; Hu, T. L.; Chen, B. J.; Yin, Z. H.; Ma, P. X.; Guo, B. L. Adhesive hemostatic conducting injectable composite hydrogels with sustained drug release and photothermal antibacterial activity to promote full-thickness skin regeneration during wound healing. *Small* **2019**, *15*, 1900046.
[32] Yin, F. X.; Yang, J. Z.; Peng, H. F.; Yuan, W. J. Flexible and highly sensitive artificial electronic skin based on graphene/polyamide interlocking fabric. *J. Mater. Chem. C* **2018**, *6*, 6840–6846.
[33] Tang, Z. H.; Yao, D. J.; Du, D. H.; Ouyang, J. Y. Highly machine-washable e-textiles with high strain sensitivity and high thermal conduction. *J. Mater. Chem. C* **2020**, *8*, 2741–2748.
[34] Li, T. K.; Chen, L. L.; Yang, X.; Chen, X.; Zhang, Z. H.; Zhao, T. T.; Li, X. F.; Zhang, J. H. A flexible pressure sensor based on an MXene-textile network structure. *J. Mater. Chem. C* **2019**, *7*, 1022–1027.
[35] Yang, S. T.; Li, C. W.; Chen, X. Y.; Zhao, Y. P.; Zhang, H.; Wen, N. X.; Fan, Z.; Pan, L. J. Facile fabrication of high-performance pen ink-decorated textile strain sensors for human motion detection. *ACS Appl. Mater. Interfaces* **2020**, *12*, 19874–19881.
[36] Pan, S. X.; Xia, M.; Fang, Z. P.; Fu, J.; Wu, Y. T.; Sun, Z. G.; Zhang, Y. H.; He, P. X. High-strength, rapidly self-recoverable, and antifatigue Nano-SiO_2/Poly (acrylamide-lauryl methacrylate) composite hydrogels. *Macromol. Mater. Eng.* **2019**, *304*, 1900130.
[37] Wei, P. L.; Chen, T.; Chen, G. Y.; Liu, H. M.; Mugaanire, I. T.; Hou, K.; Zhu, M. F. Conductive self-healing nanocomposite hydrogel skin sensors with antifreezing and thermoresponsive properties. *ACS Appl. Mater. Interfaces* **2020**, *12*, 3068–3079.
[38] Ding, Y. C.; Xu, T.; Onyilagha, O.; Fong, H.; Zhu, Z. T. Recent advances in flexible and wearable pressure sensors based on piezoresistive 3D monolithic conductive sponges. *ACS Appl. Mater. Interfaces* **2019**, *11*, 6685–6704.
[39] Lian, Y. L.; Yu, H.; Wang, M. Y.; Yang, X. N.; Li, Z.; Yang, F.; Wang, Y.; Tai, H. L.; Liao, Y. L.; Wu, J. Y. et al. A multifunctional wearable E-textile via integrated nanowire-coated fabrics. *J. Mater. Chem. C* **2020**, *8*, 8399–8409.
[40] Archana, D.; Dutta, J.; Dutta, P. K. Evaluation of chitosan Nano dressing for wound healing: Characterization, *in vitro* and *in vivo* studies. *Int. J. Biol. Macromol.* **2013**, *57*, 193–203.
[41] Sun, W. X.; Jiang, H. T.; Wu, X.; Xu, Z. Y.; Yao, C.; Wang, J.; Qin, M.; Jiang, Q.; Wang, W.; Shi, D. Q. et al. Strong dual-crosslinked hydrogels for ultrasound-triggered drug delivery. *Nano Res.* **2019**, *12*, 115–119.